Pergamon

Journal of Structural Geology, Vol. 16, No. 2, pp. 189 to 201, 1994

0191-8141/94 $06.00+0.00

Late Mozambique Belt structures in western Kenya and their influence on the evolution of the Cenozoic Kenya Rift

RALF HETZEL* and MANFRED R. STRECKER†

Geologisches Institut, Universität Karlsruhe, Kaiserstrasse 12, 7500 Karlsruhe 1, Germany

(*Received 2 September 1992; accepted in revised form 19 March 1993*)

Abstract—The N–S-trending Late Proterozoic Mozambique Belt in western Kenya is characterized by steep E-dipping foliation, generated during orogen-parallel shearing in sinistral ductile shear zones (Barsaloian event, ~580 Ma). During the final stages of orogenic evolution, two NW-trending brittle sinistral fault zones, crossing the present Elgeyo Escarpment, were active (Loldaikan event, 580–530 Ma). One of these fault zones generated well-developed pseudotachylytes that are described in detail. A later dextral reactivation of the two fault zones is related to the latest event (Kipsingian event, 530–470 Ma) of the Mozambique orogeny. Petrological, geophysical and geological data show that the Kenya Rift follows the trace of an important crustal boundary between the Archean Tanzania Craton and the Proterozoic Mozambique Belt. Miocene extensional reactivation of the steep E-dipping 'Barsaloian' foliations at the Elgeyo and Nguruman Escarpments led to the formation of asymmetric rift basins bounded by E-dipping normal faults along the western rift margin. The brittle fault zones at the Elgeyo Escarpment, trending obliquely to the basement foliation are responsible for segmentation of the Elgeyo border fault and the abrupt change in the orientation of the northern Kenya Rift.

INTRODUCTION

INHERITED crustal anisotropies are zones of weakness that often play an important role in guiding deformation during early rifting (Burke & Dewey 1973, Zoback & Zoback 1980, Cheadle *et al.* 1987, Daly *et al.* 1989, Smith & Mosley in press). For the majority of African rifts it has been shown that strike-slip and reverse faults within Proterozoic orogenic belts were reactivated during Phanerozoic rifting and influenced the location of rifts, rift propagation and the geometry of rift bounding faults (Chorowicz 1989, Daly *et al.* 1989, Fairhead & Green 1989, Versfelt & Rosendahl 1989). The East African Rift System (Fig. 1) broadly follows the trend of Proterozoic orogenic belts and is divided into a western and an eastern branch (McConnell 1972). The eastern branch follows the approximately N–S-trending Late Proterozoic Mozambique Belt in Kenya (McConnell 1972).

The location and the asymmetry of the Kenya Rift with generally E-dipping faults along the western rift margin indicates an intimate relationship between rift trend, fault geometry and pre-existing crustal structures. Well-exposed basement sections along the western margin of the Kenya Rift and a reflection of basement trends in the orientation of the rift make this region an excellent site to study the possible influence of basement structures on rifting.

The purpose of this paper is: (1) to relate the observed late orogenic deformation patterns in the Mozambique Belt to the various tectonothermal events that have been established for north-central Kenya; (2) to decipher the style and kinematics of the structures in the basement rocks along the western rift margin; (3) to show the influence of basement structures with respect to Cenozoic rifting; and (4) to differentiate Proterozoic and Cenozoic structures in the basement. The investigations were conducted along the western rift margin along the Elgeyo and the Nguruman Escarpments (Fig. 1) because of the close vicinity of basement rocks and Cenozoic rift-bounding faults.

THE EVOLUTION OF THE MOZAMBIQUE BELT

The Mozambique Belt is interpreted as the result of Tibetan-style continent–continent collision between West Gondwana (Archean Tanzania Craton) and East Gondwana (Burke & Şengör 1986, Shackleton 1986, Key *et al.* 1989, Berhe 1990). Shackleton & Ries (1984) and Shackleton (1986) suggested that collision with NW–SE relative plate motions was followed by a stage of post-collisional ductile shearing parallel to the plate boundaries. Detailed studies of Proterozoic rocks in north-central Kenya define six tectonothermal events for the evolution of the Mozambique Belt between 900 and 470 Ma (Key *et al.* 1989).

The progressive *Samburuan* and *Sabachian* (~830 Ma) tectonothermal events account for subhorizontal gneiss foliations and recumbent folding (Charsley 1987, Key *et al.* 1989). While Key *et al.* (1989) reported SE-directed thrust faulting for the Sabachian event W-vergent thrusts are documented in regions west and

*Current address: Institut für Geowissenschaften, Johannes Gutenberg Universität, Postfach 3980, 6500 Mainz, Germany.
†Current address: Department of Geology and Geophysics, School of Earth Sciences, Stanford University, Stanford, CA 94305-2115, U.S.A.

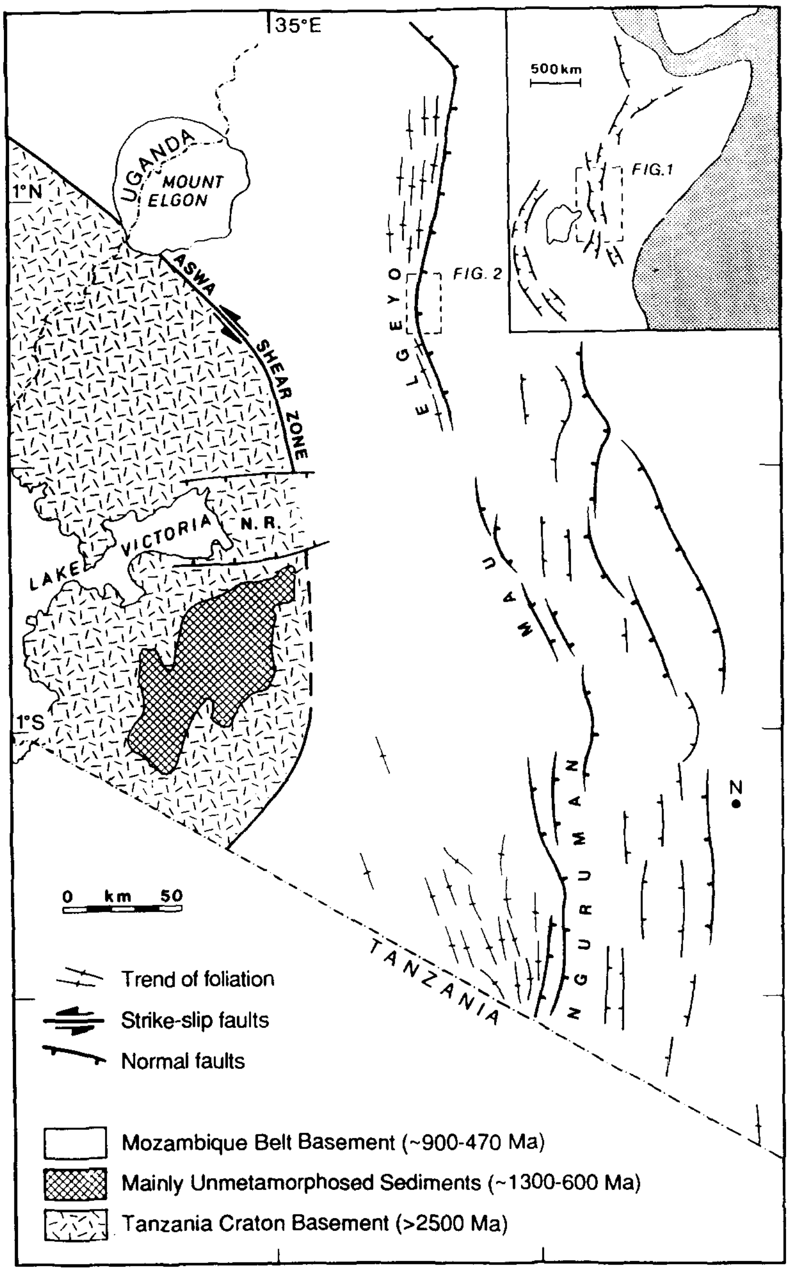

Fig. 1. Generalized geological map of Kenya with Cenozoic rift structures and major escarpments (Nguruman, Mau and Elgeyo). Inset shows location within East African Rift system. (N.R.) Nyanza Rift, Cenozoic cover rocks not shown (after Cahen *et al.* 1984, Shackleton 1986, Geological map of Kenya 1987, Key *et al.* 1989).

northwest of the Elgeyo and Nguruman Escarpments (Sanders 1963, 1965, Vearncombe 1983). Mineral assemblages indicate upper amphibolite- to granulite-facies conditions during these events. A considerable time interval separates the Sabachian from the subsequent post-collisional *Baragoian* (~620 Ma) and *Barsaloian* (~580 Ma) events. In the Mozambique Belt of Tanzania, U–Pb age determinations on zircons yielding an age of 715 Ma fall into this time interval and are interpreted to date granulite-facies metamorphism (Maboko *et al.* 1985) in the course of collision-related thickening and uplift. The Baragoian and Barsaloian amphibolite-facies events were characterized by progressively tighter folding and transposition of shallow dipping fabrics into N–S- to NNW–SSE-trending and steep E-dipping fabrics. The Barsaloian event culminated in orogen-parallel strike-slip faulting along major ductile shear zones (Key *et al.* 1989, Mathu 1992).

The ductile events were outlasted by brittle deformation with pronounced sinistral strike-slip faulting along NW–SE-trending fault zones in the *Loldaikan* (580–530 Ma) tectonothermal event (Charsley 1987, Key *et al.* 1989). These fault zones also affected the cratonic foreland of the Mozambique Belt. This is shown by the Aswa shear zone (Fig. 1) which separates undeformed Archean rocks in the west from areas characterized by W-vergent thrusts in the east (Sanders 1965). Open, asymmetric warps, trending roughly E–W, and N–S-directed compression at high tectonic levels are related to the *Kipsingian* (530–470 Ma) event which represents the final phase of isostatic uplift within the Mozambique Belt (Charsley 1987, Key *et al.* 1989).

THE BASEMENT ROCKS AT THE ELGEYO AND NGURUMAN ESCARPMENTS

Lithology

The basement rocks at the Elgeyo Escarpment consist of a wide variety of rock types. Two main types of gneisses occur but gradations between the two types are common. In addition, a basic granulite is present at the Elgeyo Escarpment east of Tambach and marbles are located further north close to Anin (Fig. 2). At the Nguruman Escarpment only felsic gneisses occur and contain abundant quartz, alkali feldspar and muscovite with variable amounts of biotite, plagioclase and sphene (Baker 1958).

Quartz–feldspar gneisses are the dominant rocks in the basement at the Elgeyo and Nguruman Escarpments. At the Elgeyo Escarpment they consist mainly of medium-grained quartz, perthitic alkali feldspar and minor amounts of plagioclase. Additionally, small amounts of orthopyroxene or clinopyroxene occur as strongly altered relics in some of these felsic gneisses. Most of the pyroxenes are replaced by medium-grained green hornblende. Fine-grained biotite is quite common and sometimes biotite has replaced hornblende.

Hornblende gneisses at the Elgeyo Escarpment contain medium-grained plagioclase, green hornblende, garnet, and usually minor amounts of quartz, perthitic alkali feldspar and biotite. Green hornblende formed at the expense of orthopyroxene and clinopyroxene which are common as relics in small amounts. At the escarpment mafic boudins of several meters length occur within the quartz–feldspar gneisses. They contain abundant garnet and clinopyroxene together with orthopyroxene, plagioclase and hornblende. The clinopyroxenes are mantled by orthopyroxene ± plagioclase whereas the garnets have been partially replaced by symplectites consisting of orthopyroxene and plagioclase.

The *basic granulite body* east of Tambach (Fig. 2) shows complex symplectite-like textures and a mineralogy that differs from all the other gneisses. Major constituents are garnet, clinopyroxene, orthopyroxene, amphibole and plagioclase. Spinel, rutile, zirkon, ilmenite and sapphirine occur as accessories. The symplectites include plagioclase, orthopyroxene and small amounts of spinel and sapphirine.

Coarse-grained *marbles* with minor amounts of quartz, feldspar, diopside and sphene occur only along the northern sections of the Elgeyo Escarpment (Fig. 2).

Metamorphic history

Evidence for the early metamorphic history of the basement is preserved by the textures in the boudins of basic composition indicating the reaction garnet + clinopyroxene ± quartz = orthopyroxene + plagioclase. The orthopyroxene–plagioclase–spinel symplectite in the granulite body at Tambach results from the reaction garnet = orthopyroxene + plagioclase + spinel. The absence of quartz indicates a more silica-deficient environment (Harley 1989). Both reactions have been described to indicate an ITD path (=isothermal decompression) in the granulite facies (Harley 1989). Rare sapphirine may have replaced kyanite by reactions similar to those described by Johansson & Möller (1986).

Comparable reaction textures in the hornblende gneisses and the granulite body indicate that the granulite body at Tambach underwent granulite-facies metamorphism together with the gneisses. The transition from granulite-facies to amphibolite-facies conditions is indicated by the appearance of green hornblende and biotite in both the quartz–feldspar and the hornblende gneisses. The availability of water during these retrograde reactions was possibly enhanced by the principal deformation event that mainly occurred during the amphibolite-facies conditions. Further retrogression was responsible for local sericitization of feldspars, which is most common near the two brittle fault zones of Tambach and Anin.

Ductile deformation

The intensity of the ductile deformation of the gneisses is dependent upon the quartz content of the rock. Lithologies rich in quartz are much more deformed than the other rock types. The granulite body near Tambach is undeformed. It is interpreted to have been emplaced in the gneisses during collision-related reverse faulting with later dismemberment during strike-slip faulting (see below). In the hornblende gneisses the foliation is only weakly developed and results from the compositional layering between layers with varying abundance in mafic minerals. The poorly developed stretching lineation is formed by hornblende crystals with a weak preferred orientation.

The foliation and stretching lineation at the Elgeyo and Nguruman Escarpments is well developed in the mylonitic quartz–feldspar gneisses. At the Elgeyo Escarpment the foliation strikes NNE to NNW and dips steeply to the east (Fig. 2). An abrupt change in the trend of the foliation occurs at 0°33′N at the intersection of the NW–SE-striking brittle Tambach fault zone (Fig. 2). North of the Tambach fault zone the foliation strikes N to NNE and the stretching lineation has a shallow S to SSE plunge (Fig. 3a). South of the fault zone the stretching lineation also has a shallow plunge to the SSE, while the foliation strikes NNW (Fig. 3b). At the Nguruman Escarpment the foliation strikes N–S and dips steeply to the east. The stretching lineation plunges to the SSE (Fig. 3c).

The well-developed mylonitic foliation comprises layers abundant in quartz or feldspar alternating with thinner layers rich in biotite, hornblende and pyroxene. The foliation planes are defined by grain boundaries of quartz and feldspar as well as by the preferred orientation of biotite, hornblende and to a lesser extent pyroxene. The foliation contains a pronounced stretching lineation comprised of quartz ribbons up to 3 cm long. Each ribbon consists of large elongate grains with well-developed subgrain boundaries indicating syntectonic recovery during relatively high temperatures (Schmid & Handy 1992). In addition to the quartz ribbons fine-grained elongate biotite flakes and hornblende constitute the stretching lineation. The biotites are affected by significant post-kinematic grain boundary migration resulting in changes of their external shape due to the prevailing high temperatures (e.g. Lister & Snoke 1984). Relatively high post-deformational tem-

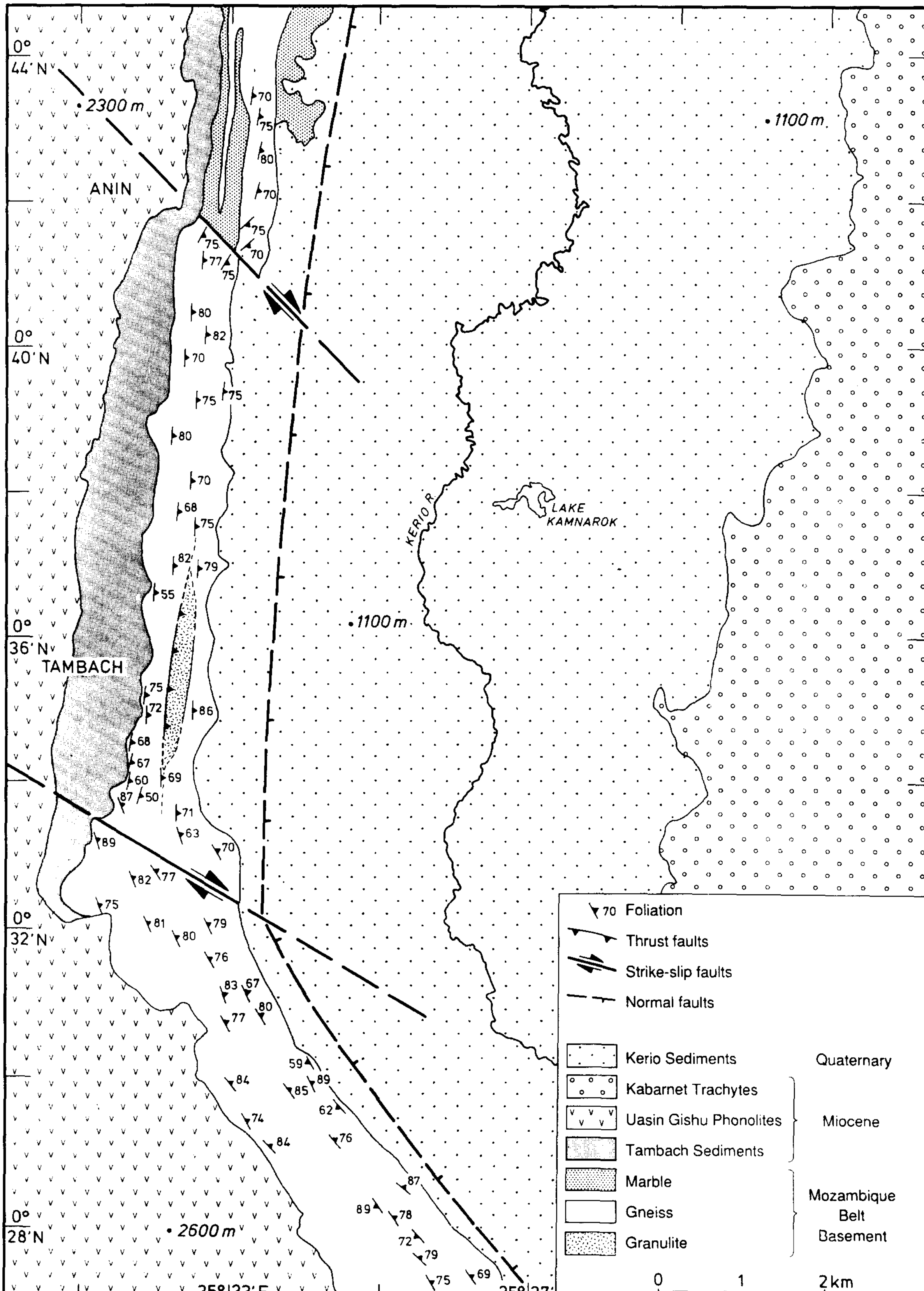

Fig. 2. Geologic map of the Elgeyo Escarpment, northern Kenya Rift (after Lippard 1972, Chapman *et al.* 1978, and authors' own observations). Dextral sense of movement along NW-striking faults corresponds to the latest event during Mozambique Belt evolution.

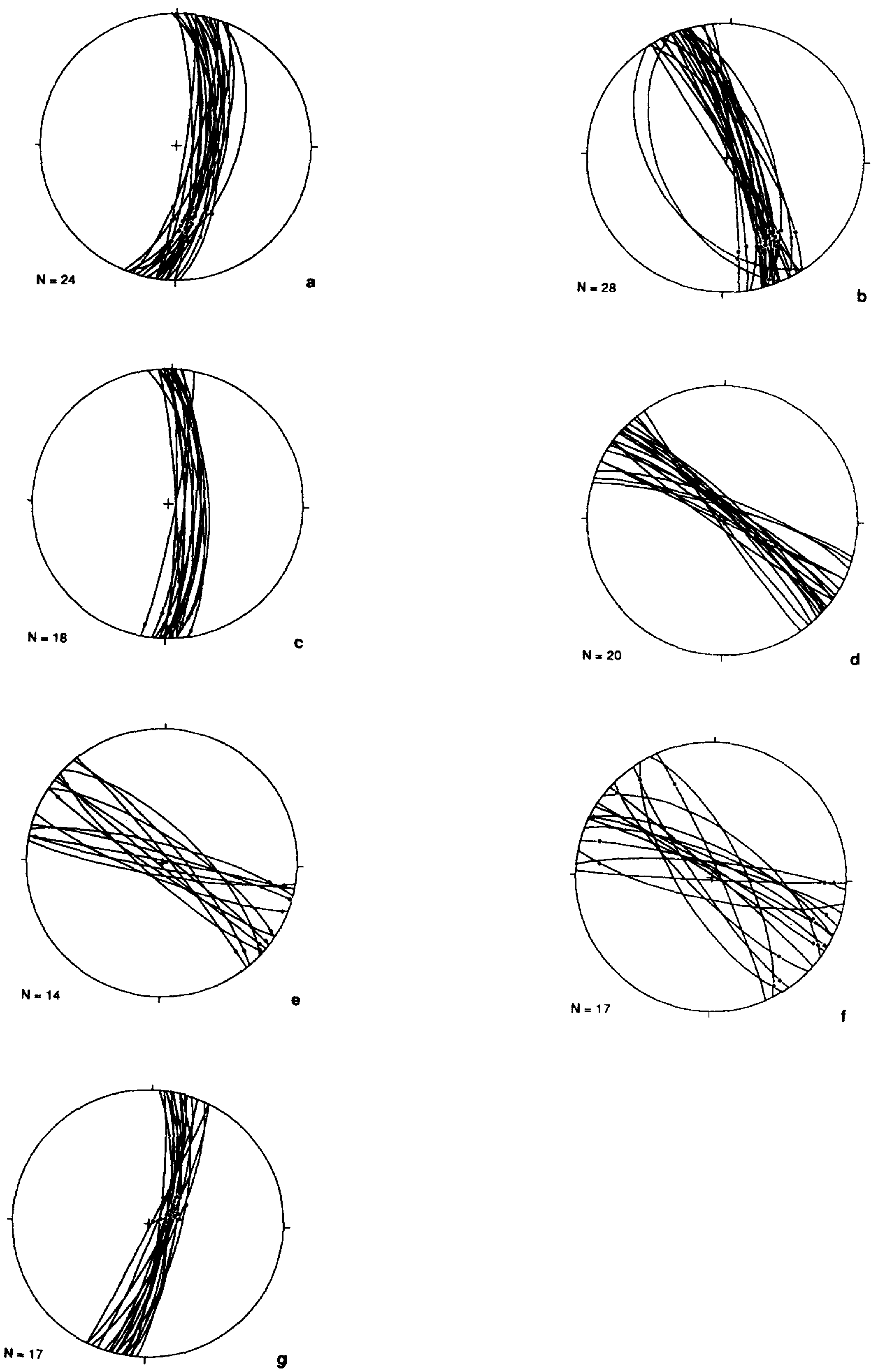

Fig. 3. Lower-hemisphere equal-area projections of foliation and stretching lineation (a–c), pseudotachylyte fault veins (d), and slickensides with striations (e–g). (a) Elgeyo Escarpment north of Tambach. (b) Elgeyo Escarpment south of Tambach. (c) Nguruman Escarpment. (d) Pseudotachylyte fault veins in the Tambach fault zone. (e) Sinistral slickensides with striations in the Tambach fault zone. (f) Dextral slickensides with striations in the Tambach fault zone. (g) Foliation-parallel slickensides with striations indicating dip-slip reactivation during rifting at the Elgeyo Escarpment east of Tambach.

peratures can also be deduced from partial static recrystallization of quartz.

The preferred orientation of biotite and hornblende as well as the syntectonic recovery of quartz show that the main deformation event occurred under amphibolite facies conditions. Preferably oriented pyroxenes are rare and may indicate the onset of ductile deformation in the granulite facies. It is assumed that the decreasing temperature during the deformation is responsible for the partial preservation of the syntectonic fabrics. Although the static recrystallization has affected the fabrics of the gneisses considerably microkinematic indicators are still recognizable. Biotite 'fish', *S–C* fabrics and asymmetric porphyroclasts of feldspar and pyroxene indicate that the basement was deformed by left-lateral shearing (Figs. 4a & b). Steep dips and shallow to moderately plunging stretching lineations in the generally N–S-trending foliation are compatible with major ductile shearing parallel to the orogen in a strike-slip regime. The lenticular shape of the undeformed granulite body at Tambach may result from the competence contrast between the granulite and the gneisses during this major ductile shearing event. The steeply-dipping contacts between the granulite body and the surrounding gneisses, as well as the dismemberment of this small granulite slice are interpreted as additional indicators of strike-slip faulting subsequent to collision.

The observed structures and fabrics are similar to the observations by Key *et al.* (1989) in the eastern parts of the Mozambique Belt of Kenya. These authors described major N–S-striking ductile shear zones in the Barsaloian (~580 Ma) event during amphibolite-facies conditions. Shackleton & Ries (1984) interpreted N–S- to NNW–SSE-trending stretching lineations in central Kenya to indicate N–S-directed relative motion parallel to the plate boundaries. South-southeast-trending stretching lineation observed at the Elgeyo and Nguruman Escarpments as well as shear sense indicators show that the Barsaloian event (~580 Ma) was characterized by left-lateral strike-slip tectonics parallel to the orogen. A roughly N–S-oriented relative motion between the Tanzania craton and East Gondwana can thus be inferred.

Collision-related strike-slip motion due to 'tectonic escape' is a general process in continental evolution and was also proposed for the Pan-African of NE and E Africa (Burke & Şengör 1986). The greenschist assemblages of volcano–sedimentary sequences and associated ophiolite complexes comprising the Arabian–Nubian Shield have been interpreted as a wedge of accreted oceanic island-arc material (e.g. Vail 1983). Subduction of the last remnants of oceanic crust in the Arabian–Nubian Shield was completed at around 500 Ma (Gass 1981). We suggest that the N–S-trending Barsaloian shear zones may reflect the tectonic escape of thickened Mozambique Belt crust along the Tanzania Craton towards the Arabian–Nubian Shield. The required sinistral motions in such a scenario would have been accommodated by the Barsaloian shear zones at the western margin of the Mozambique Belt.

Brittle deformation

Apart from the important regional ductile deformation, there are numerous brittle fault zones that traverse the Mozambique Belt basement in NE Africa (Berhe 1990). In general, these fault zones are oriented NW–SE. Along the Elgeyo Escarpment the Tambach and the Anin fault zones are the most prominent (Fig. 2), although there are numerous other fault zones that intersect the more or less meridianally trending foliation in the Mozambique Belt of Kenya (Smith & Mosley in press). These subvertical fault zones are often associated with pseudotachylyte veins (Charsley 1987, Smith & Mosley in press) that document important palaeoseismic activity (Sibson 1975, 1989). The best developed examples of pseudotachylytes are found in the Tambach fault zone.

Tambach fault zone. The black pseudotachylytes in the Tambach fault zone occur in a host rock comprised of alternating layers of hornblende and quartz–feldspar gneisses. The layers are between 1 cm and several meters thick and the pseudotachylytes occur in both lithologies. The up to 3 cm wide pseudotachylyte fault veins are recognizable with lengths between a few centimetres to more than 1 m. They are subvertical and strike uniformly NW–SE, i.e. parallel to the fault zone and oblique to the foliation (Fig. 3d). Injection veins also occur, but are much smaller and often change their trend abruptly. The geometry of pseudotachylyte fault and injection veins as well as the foliation is schematically illustrated in Fig. 6(a).

The pseudotachylytes contain between 10 and 25% porphyroclasts comprised of almost exclusively quartz, alkali feldspar, plagioclase and only minor amounts of pyroxene, hornblende and biotite. The pseudotachylyte matrix is mainly made up of plagioclase microlites up to 20 μm long, which commonly nucleated on plagioclase porphyroclasts (Fig. 4c). Flow structures (Fig. 4d) and microlites clearly indicate a melting origin (e.g. Philpotts 1964, Maddock 1986). Microlites are usually absent in thin veins and marginal contact zones with the host rock. In this case the pseudotachylytes consist of fine-grained rock-powder of cataclastic origin (Fig. 6b).

The host rock of the pseudotachylytes contains 5–10% biotite (quartz–feldspar gneiss) and 20–25% hornblende (hornblende gneiss). The scarcity of these hydrous mafic minerals in the pseudotachylytes strongly suggests that the minerals were readily assimilated during the melting process due to their low shear yield strength and their low fracture toughness (Spray 1992). Thus the pseudotachylyte melt should have contained considerable amounts of water. A water content of at least 3% in the solidified pseudotachylytes is indicated by the sums of the major element oxides in the electron microprobe analyses of the pseudotachylyte matrix which fluctuate between 94 and 97% (Hetzel 1992).

The pseudotachylytes contain no vesicles. Lithostatic pressure was therefore high enough to prevent exsolution of a vapour phase from the melt. Sibson (1975)

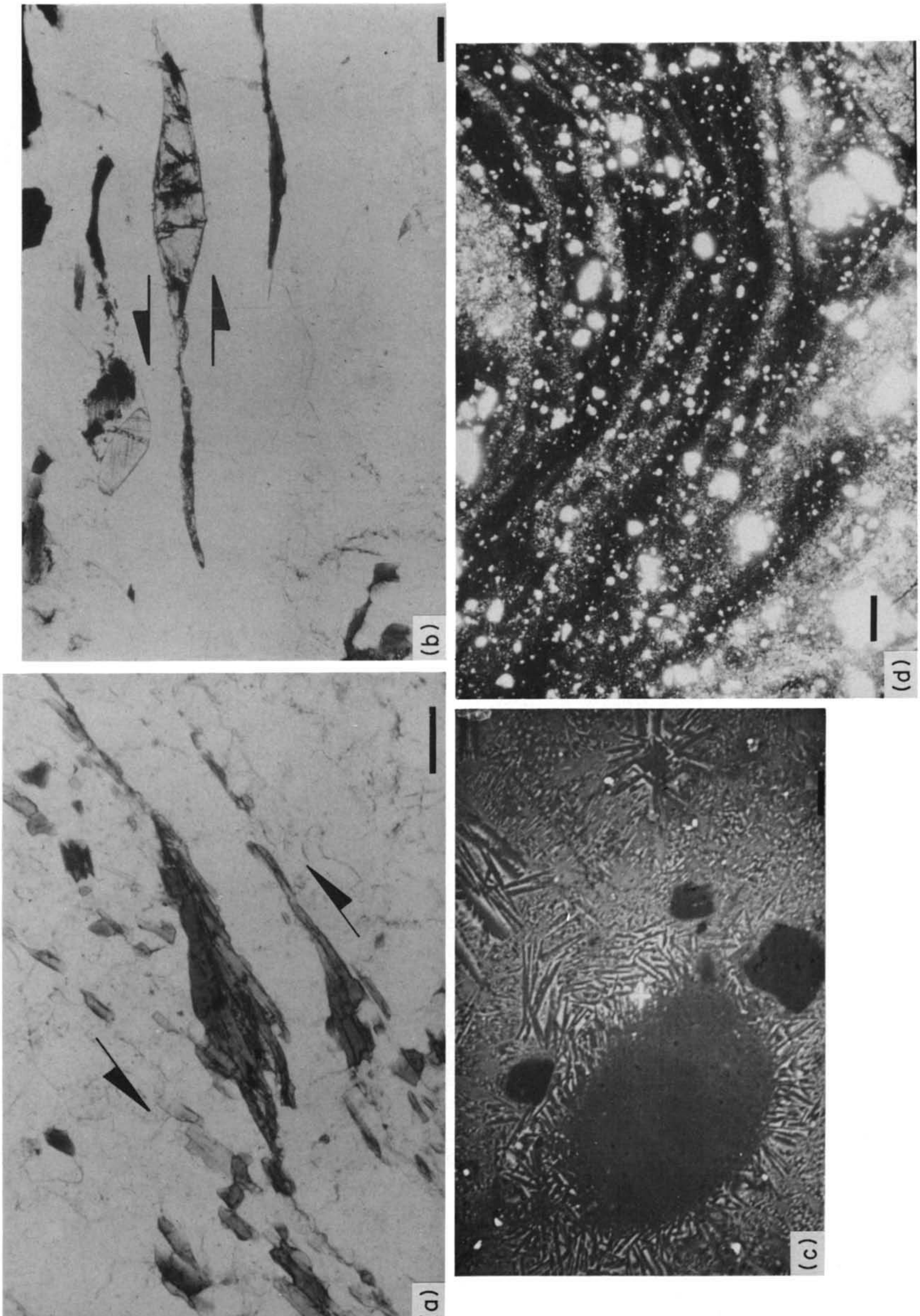

Fig. 4. (a) Biotite fish in quartz–feldspathic gneiss at the Elgeyo Escarpment, defining sinistral sense of shear (scale bar=200 μm). Arrows are aligned NNE–SSW. (b) Asymmetric pyroxene porphyroclast in quartz–feldspathic gneiss at the Elgeyo Escarpment, defining sinistral sense of shear (scale bar=200 μm). Arrows are aligned NNE–SSW. (c) BSE-photograph of microlites in pseudotachylyte matrix, Tambach fault zone. Note that microlites nucleated on the large plagioclase porphyroclast. The three dark quartz porphyroclasts were not used for the nucleation (scale bar=10 μm). (d) Flow structures in pseudotachylyte matrix. Tambach fault zone (scale bar=100 μm).

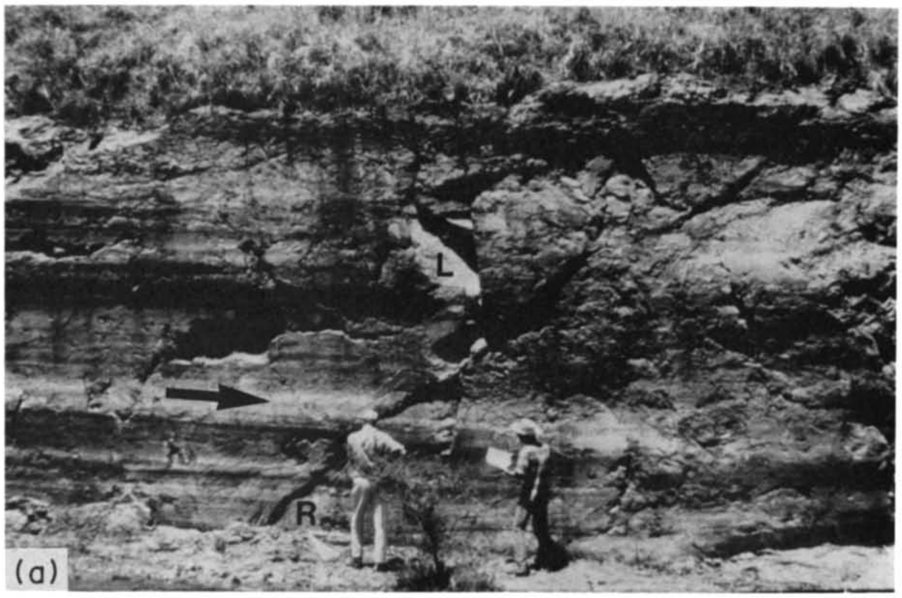

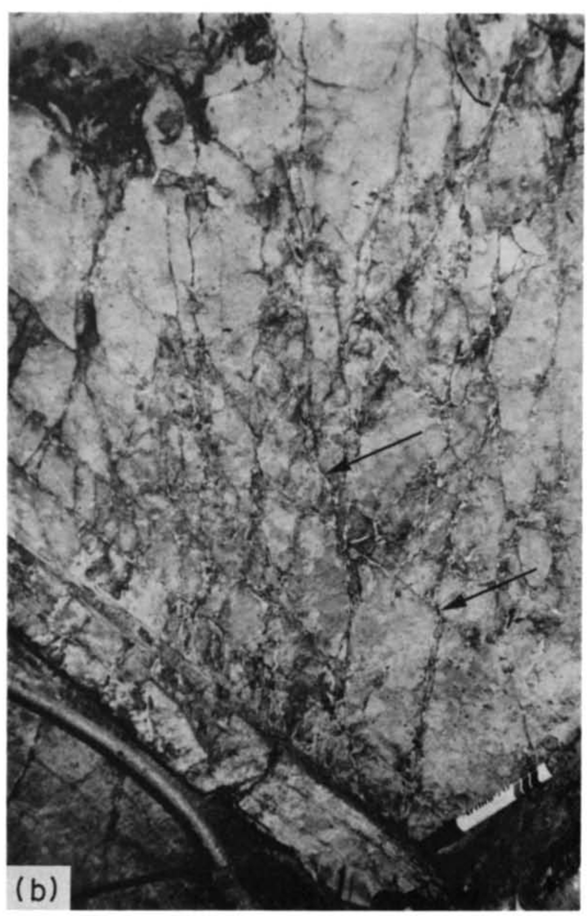

Fig. 5. (a) Large slickenside, lunate fractures (L) and Riedel shear planes (R), defining sinistral sense of shear, Tambach fault zone. Arrow shows movement direction of missing block. (b) Anastomosing subvertical tension fractures refracted at foliation discontinuities (black arrows) in gneisses at the Nguruman Escarpment.

estimated a minimum depth of 2 km for the formation of pseudotachylytes without vesicles generated in an amphibolite-facies gneiss with a water content of 1–2%. Maddock *et al.* (1987) calculated a palaeodepth of 1.6 km for pseudotachylytes containing 3% vesicles in a host rock of tonalitic gneiss with roughly 0.5% H_2O and 0.2% CO_2. For these reasons a minimum depth of at least 3 km is a reasonable estimate for the generation of the Tambach pseudotachylytes.

Field observation and inspection of thin sections show numerous sinistral shear bands that are always subparallel to pseudotachylyte fault veins (Fig. 6b). The shear bands do not offset pseudotachylyte fault veins, which suggests a coeval origin. The shear bands contain large amounts of biotite and ore indicating lower greenschist-facies metamorphism. This excludes a near-surface formation of the shear bands and the associated pseudotachylytes. In fact, the stable growth of biotite and ore suggests that the minimum depth estimate of 3 km for the generation of the pseudotachylytes may be far too shallow and a depth of ~5–8 km is a more appropriate value.

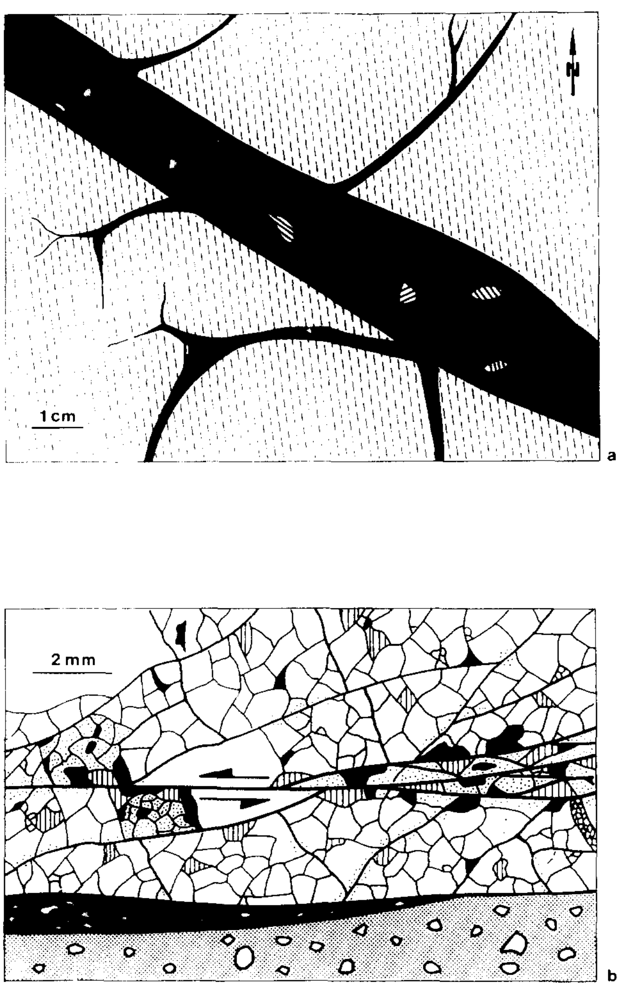

Fig. 6. (a) Sketch of the geometric relationships between foliation, pseudotachylyte fault veins, and injection veins at the Tambach fault zone. (b) NW–SE-striking pseudotachylyte fault vein. Lower part of sketch shows pseudotachylyte fault vein with cataclastic matrix (black) and matrix related to melting (stippled). For comparison see Fig. 4(c) & (e). In the centre a sinistral shear band is associated with biotite (hachures), ore (black) and Fe oxides (dots).

Two generations of slickensides with subhorizontal striations occur in the NW-striking Tambach fault zone. The first group of slickensides (Fig. 3e) has only poorly developed striations due to yellow–brown fine-grained gouge zones several millimetres thick. Riedel shears with associated lunate and crescentic fractures (e.g. Petit 1987) indicate a sinistral sense of shear (Fig. 5a). The sinistral slickensides are interpreted as the result of fault movements during aftershocks of the large earthquakes that generated the pseudotachylytes. The energy released by these aftershocks produced the fine-grained gouge on the slickensides but was too small to cause melting. Thus pseudotachylytes, shear bands and sinistral slickensides have a cogenetic relationship and are the result of seismic processes along the NW–SE-striking Tambach fault zone.

The formation of NW–SE-trending fault zones in the Loldaikan (580–530 Ma) event (Charsley 1987) and associated greenschist-facies metamorphic conditions (Key *et al.* 1989) suggest that the Tambach fault zone was initiated at this time. Charsley (1987) pointed out that due to the lack of interference structures between Barsaloian and Loldaikan structures, these two events are likely to be contemporaneous. At the Elgeyo Escarpment, however, the ductile deformation during the Barsaloian event and the brittle deformation associated with the Loldaikan event are clearly separate in time. This indicates that the two events followed each other during the uplift of the Mozambique Belt in this part of Kenya.

In contrast to the first group of slickensides associated with the pseudotachylytes, the slickensides of the second group in the Tambach fault zone show more variable trends (Fig. 3f). The subvertical slickensides are younger and are not associated with gouge layers. Microkinematic indicators document dextral displacements. North–south-directed compression at high tectonic levels has been described for the Kipsingian (530–470 Ma) event (Key *et al.* 1989). As no disruption of Cenozoic strata is visible in the vicinity of the Tambach fault zone these dextral movements are presumed to be related to this last event in the Mozambique Belt evolution (see below).

Anin fault zone. The tectonic evolution of the fault zone near Anin at 0°41'N (Fig. 2) provides further evidence for the two distinct late-stage deformation events. The Anin fault zone juxtaposes hornblende gneisses and marble. In the fault zone numerous gneiss and quartzite clasts from a few centimetres to several metres in diameter occur in a ductiley deformed matrix of pink marble. The ductile deformation of the marbles indicates temperatures of at least 200–300°C for this event (Heard & Raleigh 1972, Carter & Tsenn 1987).

We suggest that this first deformation also occurred in the Loldaikan event. The temperatures during lower greenschist-facies conditions allowed the marbles to 'flow' in a ductile manner, whereas the gneisses experienced brittle deformation. In contrast, in the gneiss-dominated Tambach fault zone this deformation event led to the formation of pseudotachylytes. Analogous to the later deformation in the Tambach fault zone, the Anin fault zone was reactivated by movements that produced subhorizontal striations in the marbles. Riedel shear planes and slickensides suggest right-lateral motion for these movements.

Similar to the dextral strike-slip deformation at Tambach, brittle deformation at Anin is also interpreted to have taken place during the Kipsingian (530–470 Ma) event. The brittle nature of the second deformation in the marble shows that movements probably took place under near-surface temperature conditions, and that it was definitely separate in time from the left-lateral movements that had created the two fault zones in the Loldaikan (580–530 Ma) event. The NW–SE-trending fault zones thus acted as zones of weakness guiding late-stage deformation in the Mozambique Belt evolution under a changed stress-field.

INHERITED ANISOTROPIES AND THE CENOZOIC KENYA RIFT

Brief history of the Kenya Rift

The Mozambique Orogeny was followed by a period of cooling, exhumation and erosion, which finally resulted in a peneplain (Saggerson & Baker 1965, Wagner 1992). In Neogene time the region was affected by volcanism and normal faulting in the course of active continental rifting in the eastern branch of the East African Rift system. Between 15 and 7 Ma half-grabens were initiated at the western boundary faults along the Elgeyo, Mau and Nguruman Escarpments (Lippard 1972, Crossley 1979, Baker *et al.* 1988). These movements occurred after widespread basalt and phonolite eruptions (e.g. Uasin Gishu Phonolites) that covered pre-rift Miocene sediments (e.g. Tambach Sediments) (Baker *et al.* 1971, Chapman *et al.* 1978). Continuing volcanic eruptions filled the initial half-graben between 7 and 5.6 Ma (e.g. Kabarnet Trachytes) before antithetic segmentation of the eastern monoclines followed in the east (Baker *et al.* 1988, Strecker 1991). The overall trend of the Kenya Rift and its relationship to basement anisotropies on both regional and local scales shows the importance of pre-existing crustal and lithospheric structure for the rifting process. A close relationship between rift bounding faults and basement structures is well illustrated along the Elgeyo and Nguruman Escarpments. These two regions are thus excellent sites in which to evaluate the influence of inherited anisotropies on Cenozoic rift faulting.

Petrological indications

On a regional scale, the vicinity of the Tanzania Craton to the west suggests an important deep-rooted crustal transition in the region of the Kenya Rift. Pickford (1982) and Smith & Mosley (in press) suggest that the rift location coincides with the eastern limit of the underthrust Tanzania Craton. The position of the cratonic margin is delineated by the occurrence of nephelinite–carbonatite volcanics, which are only found in areas with cratonic basement west of the rift (Smith & Mosley in press). According to Ashwal & Burke (1989), the different types of volcanism between the stable Tanzania Craton and the Mozambique Belt may be a function of compositional differences in the lithospheric mantle under these regions. They suggest that during Tibetan-style continental collision the depleted lithospheric mantle under the Mozambique Belt was delaminated and replaced by fertile asthenospheric mantle. With the onset of the Cenozoic thermal perturbation under East Africa the regions with fertile lithospheric mantle reacted favourably to thermal thinning of the lithosphere and generated large volumes of melt, which in turn led to widespread bimodal volcanism (Baker *et al.* 1971, Williams 1982). In contrast, the cratonic areas with depleted mantle lithosphere remained largely unaffected and caused negligible nephelinite–carbonatite volcanism (Smith & Mosley in press).

The notion of a deep crustal boundary in the vicinity of the Cenozoic rift is also supported by the ITD-path of the granulite-facies gneisses at the Elgeyo Escarpment. The simplest geological history resulting in the observed ITD-path would have involved an initial stage of crustal thickening associated with collision and subsequent heating due to thermal relaxation (e.g. England & Thompson 1984). In such a scenario isothermal decompression would have followed in the course of isostatic uplift, erosion and possibly extensional tectonics affecting the thickened crust (e.g. Harley 1989). The resulting variations of crustal composition and thickness in the collision zone thus represent potential factors controlling rifting during the onset of thermal perturbation (see below).

Geophysical indications

The effects of the spatially different asthenosphere–lithosphere dynamics in the course of active rifting are well documented by the trend of the boundary between these two layers under the inferred cratonic margin and under the Mozambique Belt (Fig. 7). According to teleseismic investigations an extremely steep boundary between the asthenosphere and lithosphere occurs immediately west of the rift; the same boundary is gentle and at a shallower position further to the east underneath the region of the Mozambique Belt (Achauer 1990, 1992, Green *et al.* 1991). The lithospheric asymmetry in the transition between Archean Craton and Mozambique Belt may therefore reflect a differential response of Archaen vs Pan-African-age lithosphere with respect to thermal perturbation during rifting (Strecker 1991, Smith & Mosley in press). Alternatively, an already existing asymmetric trend of the lithosphere–asthenosphere boundary could have been intensified by Cenozoic thermal processes. Studies on surface wave dispersion indicate pronounced variations in primary lithospheric thickness values in East Africa (Hadiouche

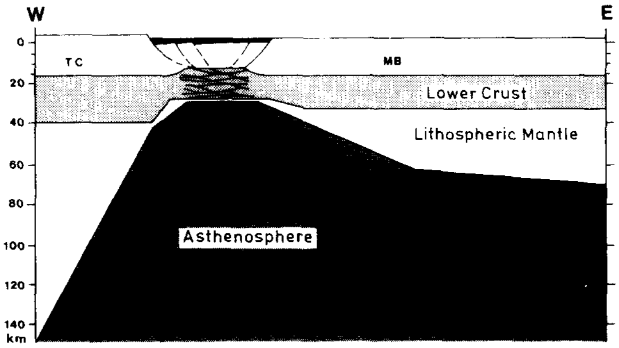

Fig. 7. Composite lithospheric E–W cross-section of the Kenya Rift. No vertical exaggeration (TC, Tanzania Craton; MB, Mozambique Belt). Simple shear in brittle upper crust is accommodated by pure shear in anastomosing shear zones in the lower crust. Modified after teleseismic observations (Achauer 1990, Green *et al.* 1991), seismic refraction profiling (KRISP 1991) and geological interpretations (Strecker 1991).

et al. 1989). Coupled with chemical differences in the upper mantle, such an asymmetry would have represented a prime site for thermally driven thinning.

The interpretation that the rift follows a boundary between the Tanzania Craton and the Mozambique Belt is also suggested by paired Bouguer gravity anomalies along the rift trend (Nyblade & Pollack 1990). An E–W seismic refraction profile encompassing both areas across the Elgeyo Escarpment and the northern Kenya Rift at about 0°40′N supports the premise of two crustal domains in this region (KRISP 1991, Mechie & Maguire in press). The crustal profile is asymmetric with up to 40 km crustal thickness west of the Elgeyo Escarpment and 35 km for the Mozambique Belt crust east of the rift. Thus rift-related crustal thinning and asthenospheric upwarp are concentrated in the transition between the two crustal domains and are characterized by pure-shear (Green *et al.* 1991). In contrast, upper crustal thinning is accommodated by simple shear deformation leading to asymmetric basins due to inherited crustal anisotropies that guided and facilitated fracture propagation.

Geological indications

Reactivation of ductile shear zones. On a local scale of individual rift basins, the important western border faults mimic the trend of the steeply E-dipping foliation which had been generated by orogen-parallel shearing during the Barsaloian tectonothermal event. Along the Elgeyo Escarpment, steeply E-dipping slickensides superposed on foliation planes document a dip-slip reactivation along foliation planes in the course of rifting (Fig. 3g). At the southern terminus of the Elgeyo Escarpment, the influence of basement foliation on the strike of Cenozoic faults is highlighted by rift-related synkinematic fluorite mineralization along fault zones within the basement rocks, overlying sediments (Kimwarer Sediments) and 15 Ma old basalts (Elgeyo Basalts). The fluorite forms ENE- to E-trending growth fibres in the plane of the steeply E-dipping basement foliation (Strecker & Smith unpublished data). The influence of the steeply-dipping basement foliation on extensional reactivation is also indicated by NNW-trending phonolitic dikes that were injected along foliation planes and traverse the overlying sediments and basalts (Strecker & Smith unpublished data).

The influence of the basement foliation on fracture propagation is further documented by tension fractures in Miocene sediments immediately south of the Tambach fault zone. The tension fractures are an integral part of foliation-parallel joint systems in the underlying basement rocks. The fractures are filled with calcite which grew at 90° to the 150–160°-striking fractures that traverse sandstones and individual basement-derived conglomerate clasts of the Miocene Tambach sediments. An ENE–WSW-oriented extension direction can thus be inferred from the tension fractures for the early rifting history at the Elgeyo Escarpment. This is in accordance with the ENE–WSW to E–W position of the extension direction during Miocene to mid-Pleistocene time in the Central Kenya Rift as derived from fault kinematic analysis and dike orientations (Strecker *et al.* 1990, Strecker & Bosworth 1991). The Pan-African Tambach fault zone juxtaposes a northern NNE- and a southern NNW-trending foliation domain. Extensional reactivation of the foliation in both areas has resulted in the pronounced change in the trend of the Elgeyo Fault (Fig. 2).

A reactivation of basement foliation is also observed along the Nguruman Escarpment in the southern Kenya Rift. There the foliation in the quartzitic and micaceous gneisses strikes between N–S and NNW and dips steeply to the east. The Nguruman Fault is characterized by a 10–40 m wide zone of fault gouge and breccia which follows the trend of the foliation (Crossley 1979). In areas where the gouge zone has been removed by erosion, anastomosing tension fractures (175–180°/85°E) traverse the basement rocks. The tension fractures are refracted at discontinuities parallel to the foliation but continue downward after several centimetres. The course of these fractures may represent a typical mode of fracture propagation and utilization of foliation planes for the formation of larger scale faults in this type of basement (Fig. 5b).

As oppposed to compressive reactivation, an extensional reactivation of anisotropies may occur over a wide range for the orientation of S_{hmin} (σ_3) (Yin & Ranalli 1992). The basement anisotropies in the region of the Kenya Rift must have been favourably oriented with respect to the prevailing stress field. Furthermore, the cohesive strength of the pre-existing structures was low resulting in extensional deformation during the onset of rifting in the Miocene.

Reactivation of brittle fault zones. While the reactivation of E-dipping foliation during rifting is evident on both regional and local scales, the reactivation of the steep NW- to NNW-trending fault zones remains equivocal. However, field observation and analysis of multispectral LANDSAT TM images in the vicinity of the Tambach and Anin fault zones do not support a reactivation of the old fault zones beyond the rift margins. Since the deposition of the Miocene Uasin Gishu Phonolites (14.5–12 Ma, Lippard 1972) and the Tambach sediments no movement has occurred along the two fault zones. This also excludes a kinematic linkage to the Aswa shear zone during rifting, which has been interpreted as a reactivated Cenozoic intra-continental transform fault (e.g. Chorowicz 1988).

The differential fault-line scarp retreat north and south of the intersection with the Anin fault zone may, however, be the trace of a Neogene transfer fault that kinematically linked spatially separate normal fault segments along the principal fault. Due to the erosional retreat of the Elgeyo Escarpment the surface expression of the hypothesized transfer fault has been covered by the Kerio Sediments (Fig. 2). In this sense the most pronounced change in the trend of the Elgeyo Escarpment at the Tambach fault zone may also be linked to a transfer fault, which acted as a kinematic link between different segments of the main bounding fault.

CONCLUSIONS

(1) Post-collisional sinistral strike-slip faulting parallel to the Mozambique Belt Orogen generated steep ductile shear zones. This resulted in the formation of steeply E-dipping foliation with shallow SSE-plunging stretching lineation at the present Elgeyo and Nguruman Escarpments.

(2) Late-stage brittle deformation in the evolution of the Mozambique Belt accounts for two important sinistral strike-slip fault zones at the present Elgeyo Escarpment trending obliquely to the foliation.

(3) On the scale of individual rift basins, the steeply-dipping foliation was reactivated by the major rift-bounding faults along the western rift margin.

(4) The brittle NW-trending fault zones are responsible for the abrupt change in rift trend at the Elgeyo Escarpment and may act as transfer faults. Large-scale reactivations of the NW-trending shear zones beyond the rift margins cannot be documented.

Acknowledgements—We appreciate the thorough reviews and suggestions made by R. Shackleton and P. Mosley. We thank H. Echtler and H. Becker for commenting on an earlier version of this paper, and E. Mathu, R. Altherr and M. Smith for discussions. P. Meier assisted with the electron microprobe work. This work was supported by a grant by the Deutsche Forschungsgemeinschaft (D.F.G.). Sonderforschungsbereich Karlsruhe (SFB 108) contribution 405. We thank the Kenya Government for research permits.

REFERENCES

Achauer, U. 1990. Das Lithosphären-Asthenosphärensystem unter dem Ostafrikanischen Rift, Kenia. Unpublished Ph.D. thesis, Universität Karlsruhe.

Achauer, U. 1992. A study of the Kenya Rift using delay-time tomography analysis and gravity modeling. *Tectonophysics* **209**, 197–207.

Ashwal, L. D. & Burke, K. 1989. African lithospheric structure, volcanism, and topography. *Earth Planet. Sci. Lett.* **96**, 8–14.

Baker, B. H. 1958. Geology of the Magadi Area. *Geol. Surv. Kenya Rep.* **42**.

Baker, B. H., Mitchell, J. G. & Williams, L. A. J. 1988. Stratigraphy, geochronology and volcano–tectonic evolution of the Kedong–Naivasha–Kinangop region, Gregory Rift Valley, Kenya. *J. geol. Soc. Lond.* **145**, 107–116.

Baker, B. H., Williams, L. A. J., Miller, J. A. & Fitch, F. J. 1971. Sequence and geo-chronology of the Kenya Rift volcanics. *Tectonophysics* **11**, 191–215.

Berhe, S. M. 1990. Ophiolites in Northeast and East Africa: implications for Proterozoic crustal growth. *J. geol. Soc. Lond.* **147**, 41–57.

Burke, K. & Dewey, J. F. 1973. Plume-generated triple junctions: Key indicators in applying plate tectonics to old rocks. *J. Geol.* **81**, 406–433.

Burke, K. & Şengör, A. M. C. 1986. Tectonic Escape in the evolution of the continental crust. In: *Reflection Seismology: The Continental Crust* (edited by Barazangi, M. & Brown, L.). *Am. Geophys. Un. Geodyn. Ser.* **14**, 41–53.

Cahen, L., Snelling, N. J., Delhal, J., Vail, J. R., Bonhomme, N. & Lendent, D. 1984. *The Geochronology and Evolution of Africa*. Clarendon Press, Oxford.

Carter, N. L. & Tsenn, M. C. 1987. Flow properties of continental lithosphere. *Tectonophysics* **136**, 27–63.

Chapman, G. R., Lippard, S. J. & Martyn, J. E. 1973. Geological map of the northern Tugen Hills. East African Geological Research Unit, Kenya Rift Valley Project, Bedford College, London.

Chapman, G. R., Lippard, S. J. & Martyn, J. E. 1978. The stratigraphy and structure of the Kamasia Range. Kenya Rift Valley. *J. geol. Soc. Lond.* **135**, 265–281.

Charsley, T. J. 1987. Geology of the Laisamis area. *Geol. Surv. Kenya Rep.* **106**.

Cheadle, M. J., McGeary, S., Warner, M. R. & Mathews, D. H. 1987. Extensional structures on the western U.K. continental shelf: A review of evidence from deep seismic profiling. *Spec. Publs. geol. Soc. Lond.* **23**, 445–465.

Chorowicz, J. 1988. Analyse de la zone de failles d'Assoua au Kenya à partir des images spatiales LAndsat-MSSS et MOMS-01. Influence de l'heritage précambrien sur la structure du Gregory Rift. *C. r. Acad. Sci., Paris* **307**, 83–88.

Chorowicz, J. 1989. Transfer and transform faults in continental rifts: examples in the Afro-Arabian Rift System. Implications of crust breaking. *J. Afr. Earth Sci.* **8**, 203–214.

Crossley, R. 1979. The Cenozoic stratigraphy and structure of the western part of the Rift Valley in southern Kenya. *J. geol. Soc. Lond.* **136**, 393–405.

Daly, M. C., Chorowicz, J. & Fairhead, J. D. 1989. Rift basin evolution in Africa: the influence of reactivated steep basement shear zones. In: *Inversion Tectonics* (edited by Cooper, M. A. & Williams, G. D.). *Spec. Publs geol. Soc. Lond.* **44**, 309–334.

England, P. C. & Thompson, A. B. 1984. Pressure-temperature-time paths of regional metamorphisms I. Heat transfer during the evolution of regions of thickened continental crust. *J. Petrol.* **25**, 894–928.

Fairhead, J. D. & Green, C. M. 1989. Controls on rifting in Africa and the regional tectonic model for the Nigeria and East Niger rift basins. *J. Afr. Earth Sci.* **8**, 231–249.

Gass, I. G. 1981. Pan-African (Upper Proterozoic) plate tectonics of the Arabian–Nubian Shield. In: *Precambrian Plate Tectonics* (edited by Kröner, A.). Elsevier, Amsterdam, 387–405.

Geological Map of Kenya. 1987. Ministry of Energy and Regional Development of Kenya.

Green, W. V., Achauer, U. & Robert, P. M. 1991. A three-dimensional seismic image of the crust and upper mantle beneath the Kenya rift. *Nature, Lond.* **354**, 199–203.

Hadiouche, O., Jobert, N. & Montagner, J. P. 1989. Anisotropy in the African continent inferred from surface waves. *Phys. Earth & Planet. Interiors* **58**, 61–81.

Harley, S. L. 1989. The origin of granulites: a metamorphic perspective. *Geol. Mag.* **126**, 215–247.

Heard, H. C. & Raleigh, C. B. 1972. Steady-state flow in marble at 500°C–800°C. *Bull. geol. Soc. Am.* **83**, 935–956.

Hetzel, R., 1992. Die Geologie des südlichen Elgeyo Escarpment (nördliches Kenia-Rift). Unpublished Diploma thesis, Universität Karlsruhe, Karlsruhe.

Johanssen, L. & Möller, C. 1986. Formation of sapphirine during retrogression of a basic high-pressure granulite, Roan, Western Gneiss Region, Norway. *Contr. Miner. Petrol.* **94**, 29–41.

Key, R. M., Charsley, T. J., Hackman, B. D., Wilkinson, A. F. & Rundle, C. C. 1989. Superimposed Upper Proterozoic collision-controlled orogenies in the Mozambique Orogenic Belt of Kenya. *Precambrian Res.* **44**, 197–225.

KRISP. 1991. Large-scale variation in lithospheric structure along and across the Kenya rift. *Nature, Lond.* **354**, 223–227.
Lister, G. S. & Snoke, A. W. 1984. S–C mylonites. *J. Struct. Geol.* **6**, 617–638.
Lippard, S. J. 1972. The stratigraphy and structure of the Elgeyo Escarpment, Southern Kamasia Hills and adjoining regions, Rift Valley Province, Kenya. Unpublished Ph.D. thesis, University of London.
Maboko, M. A. H., Boelrijk, N. A. I. M., Priem, H. N. A. & Verdurmen, E. A. T. H. 1985. Zircon U–Pb and biotite Rb–Sr dating of the Wami River Granulites, Eastern Granulites, Tanzania: Evidence for approximately 715 Ma old granulite-facies metamorphism and final Pan-African cooling approximately 475 Ma ago. *Precambrian Res.* **30**, 361–378.
Maddock, R. H. 1986. Partial melting of lithic porphyroclasts in fault generated pseudotachylytes. *Neues Jb. Miner. Abh.* **155**, 1–14.
Maddock, R. H., Grocott J. & van Nes, M. 1987. Vesicles, amygdales and similar structures in fault generated pseudotachylytes. *Lithos* **20**, 419–432.
Mathu, E. M. 1992. The Mutito and Ikoo Faults in the pan-African Mozambique Belt, Eastern Kenya. In: *Basement Tectonics, Volume* 7 (edited by Mason, R.). Kluwer, Amsterdam, 61–69.
McConnell, R. B. 1972. Geological development of the Rift System of Eastern Africa. *Bull. geol. Soc. Am.* **83**, 2549–2572.
Mechie, J. & Maguire, P. K. H. In press. A crustal and uppermost mantle cross-section through the Central Kenya Rift. *Tectonophysics*.
Nyblade, A. A. & Pollack, H. N. 1990. A new gravity model for the Gregory Rift and its western flank. *Eos* **71**, 1605.
Petit, J. P. 1987. Criteria for the sense of movement on fault surfaces in brittle rocks. *J. Struct. Geol.* **9**, 597–608.
Pickford, M. 1982. The tectonics, volcanics and sediments of the Nyanza Rift Valley, Kenya. *Z. Geomorph. Suppl. Bd* **42**, 1–33.
Philpotts, A. R. 1964. Origin of pseudotachylytes. *Am. J. Sci.* **262**, 1008–1035.
Saggerson, E. P. & Baker, B. H. 1965. Post-Jurassic erosion surfaces in eastern Kenya and their deformation in relation to rift structure. *Q. J. geol. Soc. Lond.* **121**, 51–72.
Sanders, L. D. 1963. Geology of the Eldoret area. *Geol. Surv. Kenya Rep.* **64**.
Sanders, L. D. 1965. Geology of the contact between the Nyanza Shield and the Mozambique Belt in western Kenya. *Geol. Surv. Kenya Rep.* **7**.
Schmid, S. M. & Handy, M. R. 1992. Towards a genetic classification of fault rocks: geological usage and tectonophysical implications. In: *Controversies in Modern Geology* (edited by Müller, D. W., McKenzie, J. A. & Weissert, H.). Academic Press, New York, 339–361.
Shackleton, R. M. 1986. Precambrian collision tectonics in Africa. In: *Collision Tectonics* (edited by Coward, M. P. & Ries, A. C.). *Spec. Publs geol. Soc. Lond.* **19**, 329–349.
Shackleton, R. M. & Ries, A. C. 1984. The relation between regionally consistent stretching lineations and plate motions. *J. Struct. Geol.* **6**, 111–117.
Sibson, R. H. 1975. Generation of pseudotachylyte by ancient seismic faulting. *Geophys. J. R. astr. Soc.* **43**, 775–794.
Sibson, R. H. 1989. Earthquake faulting as a structural process. *J. Struct. Geol.* **11**, 1–14.
Smith, M. & Mosley, P. In press. Crustal heterogenity and basement influence on the development of the Kenya Rift, East Africa. *Tectonics*.
Spray, J. G. 1992. A physical basis for the frictional melting of some rock-forming minerals. *Tectonophysics* **204**, 205–221.
Strecker, M. R. 1991. Das zentrale und südliche Kenia-Rift unter besonderer Berücksichtigung der neotektonischen Entwicklung. Unpublished habil. thesis, Universität Karlsruhe, Karlsruhe.
Strecker, M. R., Blisniuk, P. M. & Eisbacher, G. H. 1990. Rotation of extension direction in the central Kenya Rift. *Geology* **18**, 299–302.
Strecker, M. R. & Bosworth, W. 1991. Quaternary stress-field change and rifting processes in the East African Gregory Rift. *Eos* **72**, 17–22.
Vail, J. R. 1983. Pan-African crustal accretion in north-east Africa. *J. Afr. Earth Sci.* **1**, 285–294.
Vearncombe, F. R. 1983. A proposed continental margin in the precambrian of Western Kenya. *Geol. Rdsch.* **72**, 663–670.
Versfelt, J. & Rosendahl, B. R. 1989. Relationships between pre-rift structure and rift architecture in Lakes Tanganyika and Malawi, East Africa. *Nature, Lond.* **337**, 354–357.
Wagner, M., Altherr, R. & Van den haute, P., 1992. Apatite fission-track analysis of Kenyan basement rocks: constraints on the thermotectonic evolution of the Kenya dome. A reconnaissance study. *Tectonophysics* **204**, 93–110.
Williams, L. A. J. 1982. Physical aspects of magmatism in continental rifts. In: *Continental and Oceanic Rifts* (edited by Pálmason, G.). *Am. Geophys. Un. Geodyn. Ser.* **8**, 193–222.
Yin, Z. M. & Ranalli, G. 1992. Critical stress difference, fault orientation and slip direction in anisotropic rocks under non-Andersonian stress systems. *J. Struct. Geol.* **14**, 237–244.
Zoback, M. L. & Zoback, M. D. 1980. Faulting patterns in North-Central Nevada and strength of the crust. *J. geophys. Res.* **85**, 275–284.